Time domain BEM–FEM seismic analysis including basemat lift-off

P. N. Patel* and C. C. Spyrakos

Department of Civil Engineering, West Virigina University, Morgantown, WV 26506-6101, USA

(Received February 1989)

Strong earthquake lateral forces can induce base overturning moments that exceed the available overturning resistance due to gravity loads causing uplift of the basemat. To address the problem of uplift, a time domain BEM–FEM methodology for a two-dimensional plane strain soil–structure interaction problem is presented. The boundary element method (BEM) is applied to the soil medium and the finite element method (FEM) is applied to the foundation and the superstructure. FEM interface elements are utilized to effectively simulate foundation uplift from the underlying soil medium. The two methods are combined through displacement compatibility and force equilibrium considerations at the soil–foundation interface. A representative problem of a nuclear containment structure subjected to the El Centro earthquake of 1940 is analysed using the rigorous BEM–FEM and two approaches employing discrete models in the time and frequency domains. The results obtained from the approximate models are critically compared with those obtained from the BEM–FEM approach. The results indicate that the base shear at the foundation–structure interface can cause malevolent or benevolent effects depending on various structural and soil parameters. Further, it is concluded that the effects of uplift on the structure response cannot be predicted from the linear behaviour under bilateral contact conditions.

Keywords: seismic analysis, BEM–FEM, soil-structure interaction

Strong shaking of structures during earthquakes may result in a partial separation of the foundation basemat from the soil. The evidence of foundation uplift has been recorded by Hanson[1], after the Alaskan earthquake of March 1964, where ice was discovered under some oil tanks. Housner[2] reported the stretching of anchor bolts of a number of tall petroleum towers during the Arvin-Tehachapi earthquake, suggesting uplift of the base of the tanks from their foundations.

The response to a horizontal seismic excitation of a slender one-storey frame modelled as a single-degree-of-freedom (SDOF) system was studied by Meek[3]. Later, he extended his approach to study the dynamic behaviour of a core-stiffened, multistorey, shear building on a rigid foundation free to uplift[4]. He observed a benevolent reduction in the maximum transverse deformation and a potentially dangerous increase in the compressive forces in the columns. Kennedy *et al.*[5] determined the response of a containment building and a prestressed concrete reactor vessel placed on flexible soil. They modelled the structure using a lumped mass idealization, and the soil using translational and rotational springs with properties determined by the elastic half-space theory. An experimental, as well as an analytical, investigation of a multistorey steel frame, allowed to uplift when subjected to seismic excitation, was performed using a two-dimensional nonlinear structural analysis program by Huckelbridge and Clough[6]. They agreed with the observations made by Meek[4], and added that a reduction of the ductility, appropriately combined with uplift, can substantially reduce structural cost. Using a Winkler-Voigt soil model and a rigid foundation supported at both edges by simple springs and dashpots, Phycharis and Jennings[7] determined the response of the R.A. Millikan Library, modelled as a rigid block, when subjected to dominant seismic pulses. They found that uplift tends to reduce the rocking acceleration, but rotation can increase

* Current address: Intergraph Corporation – Rand Division, Suite 114, 17430 Campbell Road, Dallas, Texas 75252, USA.

0141-0296/90/030195-13/$03.00

or decrease depending on the excitation and the parameters of the system. Yim and Chopra[8] used a similar Winkler-Voigt soil model to obtain the response of an SDOF flexible system. They observed a reduction of structural deformations due to uplift. In their most recent work[9], they extended their formulation to analyse multistorey structures. Baba and Nakashima[10] considered the static and dynamic behaviour of a medium-rise reinforced concrete structure with flexural frames and a multistorey structural base shear wall which is allowed to uplift. They concluded that uplift can very effectively improve the seismic performance of reinforced concrete structures provided that the shear walls are designed to undertake the flexural and shear stresses developed at their bases.

A nonlinear explicit finite difference analysis using the STEALTH computer code was employed by Vaughan and Isenberg[11] to interpret the results of explosive and forced vibration field tests on small nuclear containment structures. Studies using a two-dimensional plane strain finite element idealization utilizing a Ramberg-Osgood model for maximum shear strain in each element and a constant bulk modulus for the soil were conducted by Roesset and Scaletti[12]. In their study, the excitation consisted of vertically propagating shear and dilational waves. Wolf *et al.*[13] conducted a comprehensive study for rigid circular foundations subjected to obliquely incident body waves as well as surface waves. Their analysis was based on the assumption of frequency-independent stiffness and damping soil properties. They concluded that the effects of horizontal propagating waves are greatly influenced by lift-off. Experimental and rigorous FEM studies on the effects of loss of soil-foundation contact on the dynamic response of nuclear containment structures were performed by Weidlinger Associates[14] for EPRI in relation to the SIMQUAKE II program. Such FEM analyses, however, are expensive because they require discretization of a large volume of soil under the foundation in order to avoid undesirable wave reflections at the soil boundaries. Antes and Steinfeld[15] determined the response of a dam allowed to uplift from the underlying soil media subjected to externally applied impulsive vertical and horizontal loads. In their analysis, both the dam and the soil media were modelled with a time domain boundary element method (BEM). Hillmer and Schmid[16] obtained response of a building allowed to uplift utilizing a Laplace domain technique, in which the structure was idealized with beam elements utilizing continuous mass distribution and BEM was applied to model the soil media. The nonlinearities were dealt with in the time domain, while all other calculations took place in the Laplace domain.

The approach considered in this work extends the hybrid time domain BEM-FEM methodology developed by Spyrakos and Beskos[17] and Karabalis and Beskos[18], who studied the dynamic response of two- and three-dimensional foundations in complete bond with the soil. In their works the BEM-FEM formulation employed the BEM to model semi-infinite soil media and the finite element method (FEM) to model the finite domain of the structure and the foundation. The BEM is particularly well suited to model soil domains because of its ability to automatically account for the radiation conditions at infinity, and reduces the spatial dimensions of the problem by one[19,20]. The expressions presented in this work allow the treatment of elastodynamic problems involving partial loss of contact between elastic bodies as is exemplified through a representive soil-structure interaction (SSI) problem. Further, the methodology incorporates FEM interface elements to model the foundation-soil contact area to investigate the effects of the nonlinearities arising from the soil-foundation separation. The BEM-FEM model is employed to determine the response of a representative nuclear containment building subjected to El Centro earthquake of 1940 under unilateral contact (uplift permitted) with the soil media. Two approximate discrete models are also presented in the time and frequency domains to gauge their accuracy over the rigorous BEM-FEM approach. The three approaches, the rigorous BEM-FEM model and the approximate models, are critically compared and design recommendations are given. A parametric study is also conducted for the parameters that most characterize structural behaviour, i.e., mass, stiffness, and height of the foundation-structure system.

BEM-FEM formulation

BEM formulation

Under the assumption of small displacement theory and homogeneous, isotropic, linear elastic material behaviour, the elastodynamic displacement field $u_i(x, t)$ of a body under conditions of plane strain is governed by Navier's equation

$$(c_1^2 - c_2^2)u_{j,ii} + c_2^2 u_{i,jj} - \ddot{u}_i = -\frac{1}{\rho} b_i \,(i, j = 1, 2) \qquad (1)$$

where commas and dots indicate space derivatives and the time derivatives, respectively, ρ is the mass density of the material and b_i are the components of the body force distribution in the domain Ω. The propogation velocities of the pressure and shear waves denoted as c_1 and c_2, respectively, are given in terms of the Lame's constants λ and μ by

$$c_1 = \sqrt{\frac{\lambda + 2\mu}{\rho}} \quad \text{and} \quad c_2 = \sqrt{\frac{\lambda}{\rho}} \qquad (2)$$

In a well posed boundary value problem, equation (1) must be accompanied by appropriate initial conditions

$$u_i(x, t) = \bar{u}_{i_0}(x)$$

$$\dot{u}_i(x, t) = \bar{v}_{i_0}(x) \text{ for } t = t_0 \text{ in } \Omega + T \qquad (3)$$

and boundary conditions

$$u_i(x, t) = \bar{u}_i(x, t) \text{ for } t > t_0 \text{ on } T_1$$

$$t_i(x, t) = \bar{T}_i(x, t) \text{ for } t > t_0 \text{ on } T_2 \qquad (4)$$

where $T = T_1 + T_2$ and Ω denote the boundary and the interior of the domain, respectively, and the bar indicates that the values are known.

For zero body forces and zero initial conditions, the initial-boundary value problems defined by Navier's equation and the associated boundary and initial conditions can be expressed by the integral equations[21]

$$\frac{1}{2} u_j(\xi, t) = \oint_T (U_j^{(i)} * t_{(i)j} - T_j^{(i)} * u_j) dT \qquad (5)$$

where $t_{(\eta)j}$ are the surface tractions, the operation * denotes time convolution and the fundamental tractions, $T_j^{(i)}$, corresponding to the fundamental displacements

$$U_j^{(i)}(x, \xi; t') = \frac{1}{2\pi\rho}\left\{\frac{1}{c_1}\frac{H(c_1t'-r)}{2} \times\left[\frac{2c_1^2t'^2-r^2}{R_1}r_{,i}r_{,j}-R_1\delta_{ij}\right] -\frac{1}{c_2}\frac{H(c_2t'-r)}{r^2} \times\left[\frac{2c_2^2t'^2-r^2}{R_2}r_{,i}r_{,j} -\left(R_2+\frac{r^2}{R_2}\right)\delta_{ij}\right]\right\} \quad (6)$$

$$R_\alpha = \sqrt{(c_\alpha^2t'^2-r^2)},\ \alpha = 1, 2$$

$$t' = t - \tau \quad (7)$$

are given in Patel[22]. In the fundamental solution, H denotes the Heaviside function, and r is the distance $|x - \xi|$ between a field point x and a source point ξ.

Equation (5) can be applied to obtain the displacement response at the boundary of an elastic body. Once the boundary value problem is solved, the displacements and tractions in the interior of the domain Ω can be easily evaluated in terms of the response obtained on the surface[19,20]. A solution of the integral equation (5) in closed form for general conditions is not possible; thus resort is made to numerical solution. The numerical treatment is accomplished through spatial and time interpolations of the displacement and traction fields. More specifically, the boundary T is discretized into Q line elements, while the time variation of the displacements and tractions over each element are assumed to be constant during each time step. The displacement at the centre of the element P at the time step N is given by the following discretized form of equation (5)[17]

$$c_{ij}u^{NP} = \sum_{q=1}^{Q}\sum_{n=1}^{N}\left(\left[\int_{\Delta S}G_{ij}^{nq}ds\right]\{t^{N-l+1}\} -\left[\int_{\Delta S}F_{ij}^{nq}ds\right]\{u^{N-l+1}\}\right) \quad (8)$$

where $l = n - m + 1$, G_{ij} and F_{ij} are the discretized fundamental displacements and tractions, respectively. In evaluating the line integrals of the fundamental solution pair, singularities appear when p is equal to q in equation (8) for every time step N. A detailed evaluation of these singularities is presented in Reference 22. In the next subsection, the expressions resulting from the application of equation (8) to every boundary element is combined through appropriate compatibility with the FEM interface element equations to perform an iterative numerical treatment of the nonlinearities due to the soil-foundation uplift.

FEM formulation

The foundation and structure are modelled with the aid of FEM. The four node plane strain bilinear rectangular elements with two degrees of freedom per node shown in *Figure 1* are used in this study. Through standard FEM

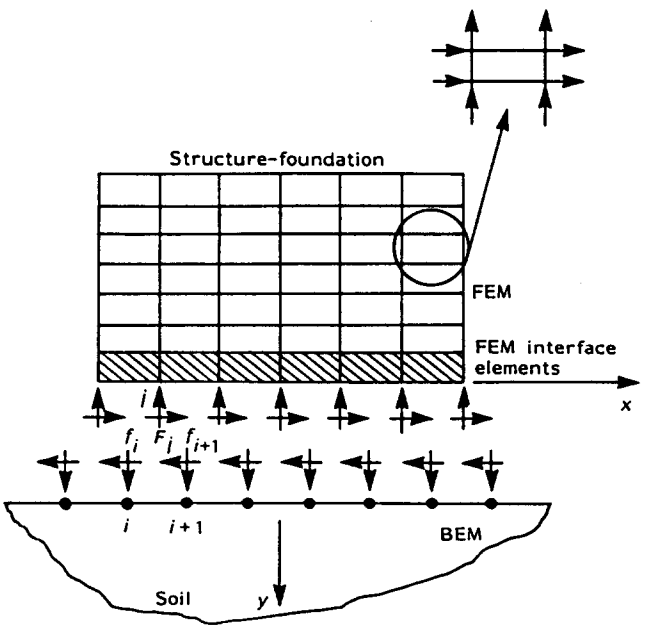

Compatibility considerations

Force equilibrium	Displacement compatibility
$F_j = \frac{1}{2}f_i + \frac{1}{2}f_{i+1}$	$\delta_j = \frac{1}{2}u_i + \frac{1}{2}u_{i+1}$

Figure 1 BEM-FEM force and displacement compatibility considerations

procedures, the following equations of motion can be obtained by an assemblage of the individual finite elements[23,24]

$$[M]\{\ddot{\delta}\} + [C]\{\dot{\delta}\} + [K]\{\delta\} = \{f(t)\} \quad (9)$$

where δ indicates nodal displacements. $[M]$, $[C]$ and $[K]$ are the consistent mass, damping and stiffness matrices of the foundation-structure system, respectively, and $\{f(t)\}$ is the nodal force vector.

The geometric nonlinearities considered herein result from the time-dependent nature of the contact area between the soil and the foundation when uplift occurs. To treat these nonlinearities effectively, thin layer four node bilinear rectangular interface elements are used to discretize the soil-foundation interface. The three modes of deformation that accurately simulate the uplift of the foundation basemat are the stick, debonding and rebonding modes. An interface element is in the stick mode when there is no relative motion between the adjoining bodies and no tensile stresses are developed due to the external disturbances. Separation or debonding takes place when the bodies open up due to constraints of unilateral contact conditions, prohibiting the development of tensile stresses as they are incompatible with constitutive properties of the geologic materials. If the interface element in the debonding mode returns to the stick mode during subsequent loading, rebonding takes place. Interface elements similar to the one described above have been successfully used to solve static as well as dynamic two-dimensional problems, where all domains have been discretized with the aid of FEM[25,26]. In this study, the equations of the interface elements are derived separately and then added to those of the foundation-structure system prior to establishing the compatibility and equilibrium criteria with soil BEM modelling.

The aspect in which the inteface elements differ from regular elements, such as the ones used to model the superstructure, is their thickness ratio

$$t_r = \frac{t_{\text{int}}}{t_{\text{neigh}}}$$

where subscripts int and neigh pertain to the interface and the neighbouring regular FEM element, respectively. The small value of thickness of the interface element is liable to cause numerical problems; however, Pande and Sharma[26] suggests guidelines that can be followed to circumvent the numerical problems. In this study, a thickness ratio of 0.1 has lead to convergent results.

The stick mode of deformation is treated like any other regular FEM element with material properties which are identical to those of the underlying soil media. The additional stiffness and inertia introduced in the system are negligible considering the semi-infinite soil media laying underneath the interface elements. The Young's modulus of elasticity is reduced for the interface element in the debonding mode by

$$[D]_{\text{debonding}} = 0.001 \times [D]_{\text{stick}} \tag{11}$$

where $[D]_{\text{stick}}$ is the material property matrix in the stick mode. This, in essence, creates a void element with very little stiffness. In the rebonding mode, the material properties corresponding to the soil media are reassigned, which brings back the interface element to the stick mode. More information on the complete implementation of the interface elements in the BEM-FEM methodology can be found in Reference 22.

Time-stepping algorithm

The two approaches, BEM and FEM, are coupled appropriately by displacement compatibility and force equilibrium considerations at the soil-foundation interface. The displacements of the BEM soil elements are evaluated at the midpoint, while the FEM displacements correspond to the FEM nodes as shown in *Figure 1*. In order to introduce compatibility between the deformations of the interface element nodes and the soil motion, the average displacement of FEM node q is approximated by the mean value of the nodal displacements at the ends of the BEM element p. Similarly, compatibility of forces can be established if each contact force f_q applied at node q is approximated by the mean value of the two resultant forces P associated with the contact stresses that develop over two successive elements joined at their common node. Thus, for the whole interface region, the compatibility relationships can be expressed as

$$\{\delta\} = [T]\{u\} \tag{12}$$

$$\{F\} = [T]\{f\} \tag{13}$$

where $[T]$ is the transformation matrix composed of zero and 1/2 entries. In view of equations (12) and (13), equation (8) of BEM formulation can be expressed as

$$[T]^T[\bar{B}] = [T]^T[B][T]\{\delta\} \tag{14}$$

where

$$[B] = \frac{l}{2}[G^1]^{-1} \tag{15}$$

and

$$[\bar{B}] = l[G^1]^{-1}([G^2]\{t^{N-1}\} + [G^3]\{t^{N-2}\} + \cdots + [G^N]\{t^1\}) - ([H^2]\{u^{N-1}\} + [H^3]\{u^{N-2}\} + \cdots + [H^N]\{u^1\}) \tag{16}$$

in which superscripts denote the time steps at which the quantities are evaluated and l represents the length of the element. It should be noted that equation (16) represents the time convolution process stipulated in equation (8), and indicates that the matrix $[\bar{B}]$ depends on the complete time history prior to the time step at which it is evaluated. Combining the BEM and FEM formulations results in the set of nonlinear equations governing the response of the soil-structure system:

$$[M_t]\{\ddot{\delta}\} + [C_t]\{\dot{\delta}\} + [\bar{K}_t]\{\delta\} = \{F(t)\} \tag{17}$$

where the subscript of t denotes the time-dependent nature of the matrices arising from the changing contact area at the soil-foundation interface; $[M_t]$ and $[C_t]$ are the mass and damping matrices, respectively; $[\bar{K}_t]$ is the equivalent stiffness matrix given by

$$[\bar{K}_t] = \begin{bmatrix} [K] + [T]^T[B_{cc}][T] & [T]^T[B_{ce}][T] \\ [T]^T[B_{ec}][T] & [T]^T[B_{ee}][T] \end{bmatrix} \tag{18}$$

and the time-dependent forcing function $F(t)$ can be evaluated from

$$F(t) = \begin{bmatrix} [T]^T[\bar{B}_{cc}][T] + [K] & [T]^T[\bar{B}_{ce}] \\ [T]^T[\bar{B}_{ec}][T] & [\bar{B}_{ee}] \end{bmatrix} \begin{Bmatrix} \{\delta_c^f\} \\ \{u_e^f\} \end{Bmatrix} \tag{19}$$

where the superscript f denotes the free-field, and subscripts c and e represent the degrees of freedom corresponding to the foundation-soil contact area and the external discretization on either side of the contact area, respectively. The nonlinear system of equations (17) is solved with the aid of the direct integration scheme presented in the Appendix. A flowchart depicting the procedure followed for evaluation of the contact area and the structure response is shown in *Figure 2*. Initially the foundation and the soil are assumed to be in complete bond. For each time step an iterative procedure is employed to determine the size of the correct contact area. More specifically, if at the end of a given iteration the contact area is not the same as the one assumed at the beginning of the iteration, a new contact area is computed based on the displacements found in the current iteration. The procedure is repeated until convergence that renders the contact area.

Approximate analysis

Two approximate models in the time and frequency domain are presented to assess the accurary of the BEM-FEM time domain methodology. The models are utilized to obtain the response of a nuclear containment building subjected to a seismic excitation under either bilateral (complete bond) or unilateral contact (uplift permitted) conditions.

Time domain approximate model

The structure is idealized as a rigid block with mass M and mass moment of inertia I_{0x} resting on a set of horizontal and vertical spring-dashpot system, as shown in *Figure 3*. The equations governing the motion of the structure for two conditions of contact between the

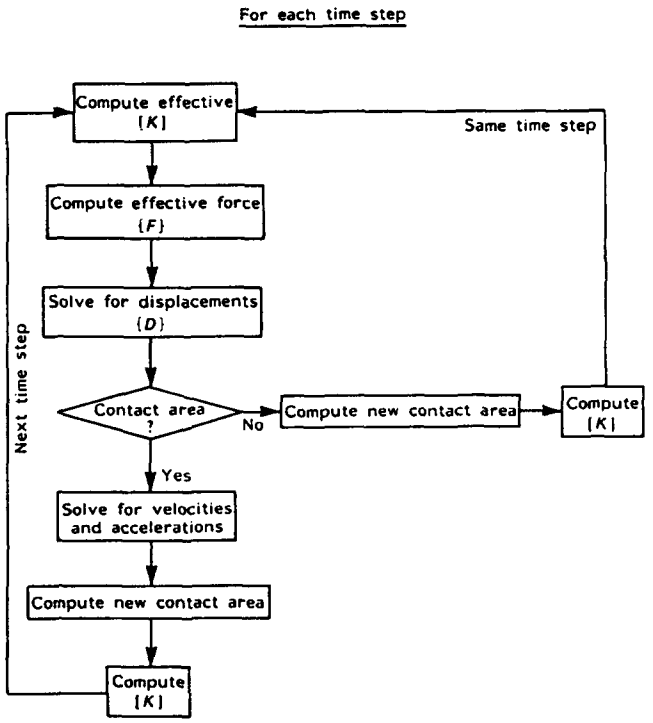

Figure 2 Flowchart of the iterative algorithm for BEM–FEM analysis

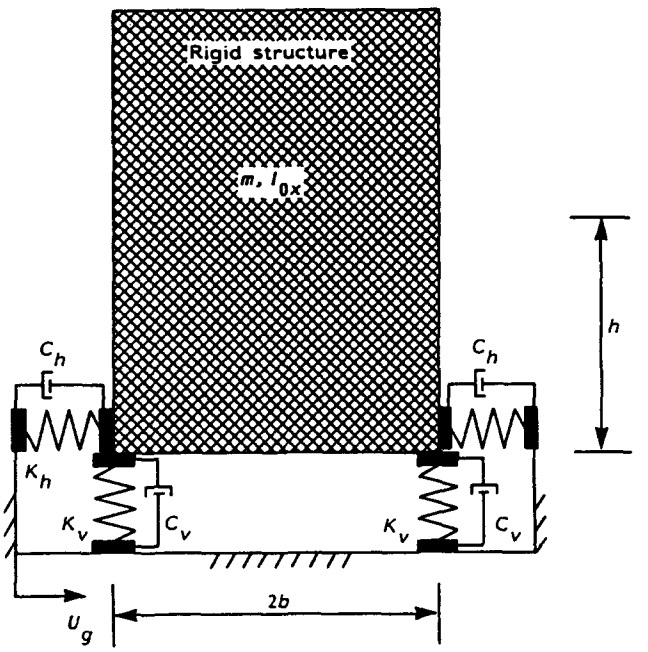

Figure 3 Time domain approximate model

foundation and soil, bilateral and unilateral, are presented. These equations are derived under the assumption that the structural response amplitudes are small for seismic excitation. The governing equations resulting from the lateral, vertical and moment equilibrium of the forces acting on the entire system are given by[22]

$$\begin{bmatrix} m & m & 0 \\ m & \frac{I_{0x}}{h^2}+m & 0 \\ 0 & 0 & m \end{bmatrix} \begin{Bmatrix} \ddot{u} \\ h\ddot{\phi} \\ \ddot{v} \end{Bmatrix} + \begin{bmatrix} \varepsilon_1 C_h & 0 & 0 \\ 0 & \varepsilon_1 \frac{b^2}{h^2} C_v & \varepsilon_2 \frac{b}{h} C_v \\ 0 & \varepsilon_2 \frac{b}{h} C_v & \varepsilon_1 C_v \end{bmatrix} \begin{Bmatrix} \dot{u} \\ h\dot{\phi} \\ \dot{v} \end{Bmatrix} + \begin{bmatrix} \varepsilon_1 K_h & 0 & 0 \\ 0 & \varepsilon_1 \frac{b^2}{h^2} K_v - \frac{mg}{h} & \varepsilon_2 \frac{b}{h} K_v \\ 0 & \varepsilon_2 \frac{b}{h} K_v & \varepsilon_1 K_v \end{bmatrix} \times \begin{Bmatrix} u \\ h\phi \\ v \end{Bmatrix} = \begin{Bmatrix} -m\ddot{u}_g \\ -m\ddot{u}_g \\ -mg \end{Bmatrix} \tag{20}$$

where

$$\varepsilon_1 = \begin{cases} 2 & \text{both edges in contact} \\ 1 & \text{one edge uplifted} \end{cases}$$

$$\varepsilon_2 = \begin{cases} -1 & \text{left edge uplifted} \\ 0 & \text{both edges in contact} \\ 1 & \text{right edge uplifted} \end{cases} \tag{21}$$

For the case of plane strain, the spring stiffnesses of the elastic half-space are approximated by the following frequency-independent expressions[28,29]

$$K_v = 0.5\pi \frac{G_s b}{1-\nu_s} \tag{22}$$

and

$$K_h = 0.35\pi \frac{G_s}{2(1-\nu_s)} \tag{23}$$

where G_s and ν_s are the shear modulus and Poisson's ratio of the soil, respectively, and b is the half base width of the foundation. The following expressions of the frequency-independent damping coefficients C_v and C_h are used to approximate radiation damping in the soil

$$C_v = 1.17\pi\rho_s c_2 b \tag{24}$$

and

$$C_h = \frac{0.72\pi\rho_s c_2 b}{2} \tag{25}$$

The motion of the structure under bilateral contact conditions is governed by the linear differential equations (20) for $\varepsilon_1 = 2$ and $\varepsilon_2 = 0$. Under unilateral contact conditions, the governing differential equations are nonlinear, since the boundary conditions change with time. The transition from no uplift to uplift can be detected by the presence of a tensile force in the vertical spring and a displacement in the upward direction. Within each time step, the instant of transition from stick to uplift or uplift to stick is obtained by an iterative procedure. Although a closed form solution of equation (20) can be obtained for simple excitations, numerical implementation would be necessary for complicated earthquake-like excitations. The solution algorithm implemented herein is that of Newmark's direct integration scheme for nonlinear problem[27].

Frequency domain approximate model

The containment structure is modelled as a rigid block supported by a horizontal and rotational spring-dashpot system as shown in *Figure 4*. This simple model is developed to determine the structure's response under bilateral contact conditions with the aid of response spectra. The equations of motion governing the harmonic horizontal and rocking response of the system are

$$\begin{bmatrix} \frac{\omega_h^2}{\omega^2}(1+2\xi_h i)-1 & -1 \\ -1 & \left(\frac{\omega_r^2}{\omega^2}(1+2\xi_r i)-1\right)\left(1+\frac{I_{0x}}{h^2 m}\right) \end{bmatrix} \times \begin{Bmatrix} u_0 \\ h\phi \end{Bmatrix} = \begin{Bmatrix} u_g \\ u_g \end{Bmatrix} \tag{26}$$

where ξ_h and ξ_r represent the damping ratios characterizing the radiation damping for the horizontal and rocking motions, respectively, and the natural frequencies ω_h and ω_r are expressed by

$$\omega_h = \sqrt{\frac{K_h}{m}} \quad \text{and} \quad \omega_r = \sqrt{\frac{K_r}{m}} \tag{27}$$

The horizontal spring stiffness and damping coefficient can be obtained from equations (23) and (25); however, the values must be doubled since there is only one spring-dashpot system characterizing the soil flexibility in the horizontal direction as shown in *Figure 4*. The rocking spring stiffness and the damping coefficient for the case of plane strain can be approximated by the following equations[28,29]

$$K_r = 0.5\pi \frac{G_s b^2}{1-\nu_s} \tag{28}$$

$$C_r = 0.19\pi \frac{\rho_s c_2 b^3}{1-0.8\nu_s} \tag{29}$$

The natural frequencies ω_1 and ω_2 of the two-degrees-of-freedom system can be evaluated from equation (26) as

$$\omega_{1,2}^2 = \frac{1}{2}\left(1+\frac{h^2 m}{I}\right)(\omega_h^2+\omega_r^2) \times \left[1 \pm \sqrt{1-\frac{4}{h^2(m/I)+1}\frac{\omega_h^2\omega_r^2}{(\omega_h^2+\omega_r^2)^2}}\right] \tag{30}$$

The soil-structure system does not have classical modes of vibration; that is, the transformation to modal coordinates does not decouple the damping terms. Therefore, this model is used to approximate the fundamental frequency of the system, which in turn is used to evaluate the response amplitude of the structure system to the El Centro earthquake with the aid of the response spectra shown in *Figure 5b*.

The fundamental natural frequency of the system used in the approximate analysis has been determined by setting all damping terms ξ_h and ξ_r equal to zero in equation (26).

$$\omega_1 = \sqrt{\frac{\omega_h^2\omega_r^2}{\omega_r^2+\omega_r^2}} \tag{31}$$

Following the energy considerations outlined by Wolf[27], the damping ratio that should be used in conjunction with ω_1 to determine the response of the equivalent SDOF system through the response spectra is given by

$$\xi_1 = \frac{\omega_1^2}{\omega_h^2}\xi_h + \frac{\omega_1^2}{\omega_r^2}\xi_r \tag{32}$$

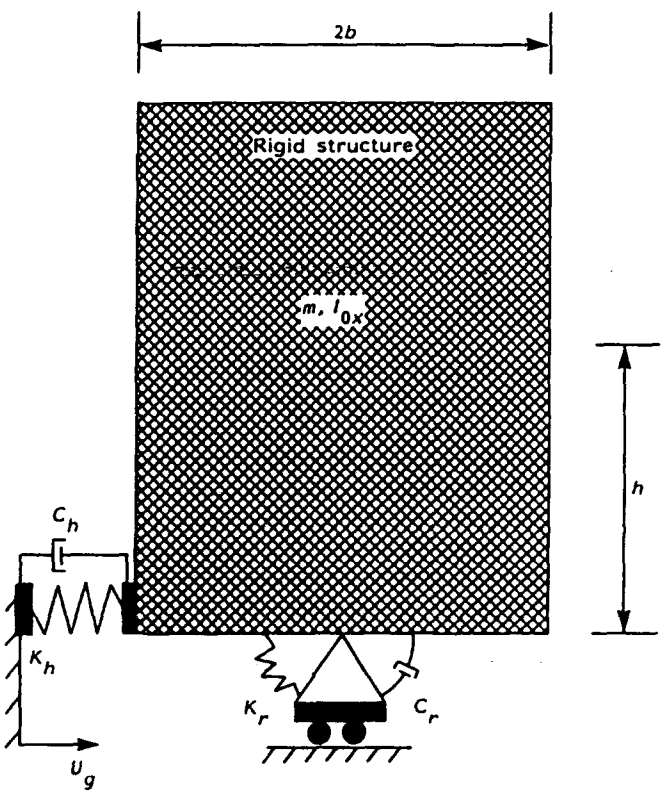

Figure 4 Frequency domain approximate model

Numerical example

The time domain BEM-FEM methodology and the approximate models are employed to obtain the response of a nuclear containment structure subjected to the horizontal component of the El Centro earthquake of 1940. The containment structure has been studied by Weidlinger Associates (1982) in their study for EPRI, in which they conducted experimental and analytical FEM soil-island analyses for blast loading arising from buried explosives. The soil is characterized by a shear wave velocity of 650 ft/s and a pressure wave velocity of 1300 ft/s, while a modulus of elasticity $E_f^o = 106\,560\,369$ lb/ft^2, Poisson's ratio $\nu_f = 1/3$ and mass density $\rho_f^o = 3.04348$ lb-s^2/ft^2 are taken to be material properties of the foundation elements. The superstructure is characterized by a modulus of elasticity $E^o = 106\,577\,648$ lb/ft^2, Poisson's ratio $\nu = 1/3$ and mass density $\rho^o = 0.59006$ lb-s^2/ft^2. The variation of the foundation and superstructure material properties for the parametric study are presented in *Table 1*. The equivalent two-dimensional plane strain model and its BEM-FEM discretization are shown in *Figure 6*. The soil surface is discretized into 10 BEM elements at the soil-foundation contact area and five BEM elements on either side of the foundation. This

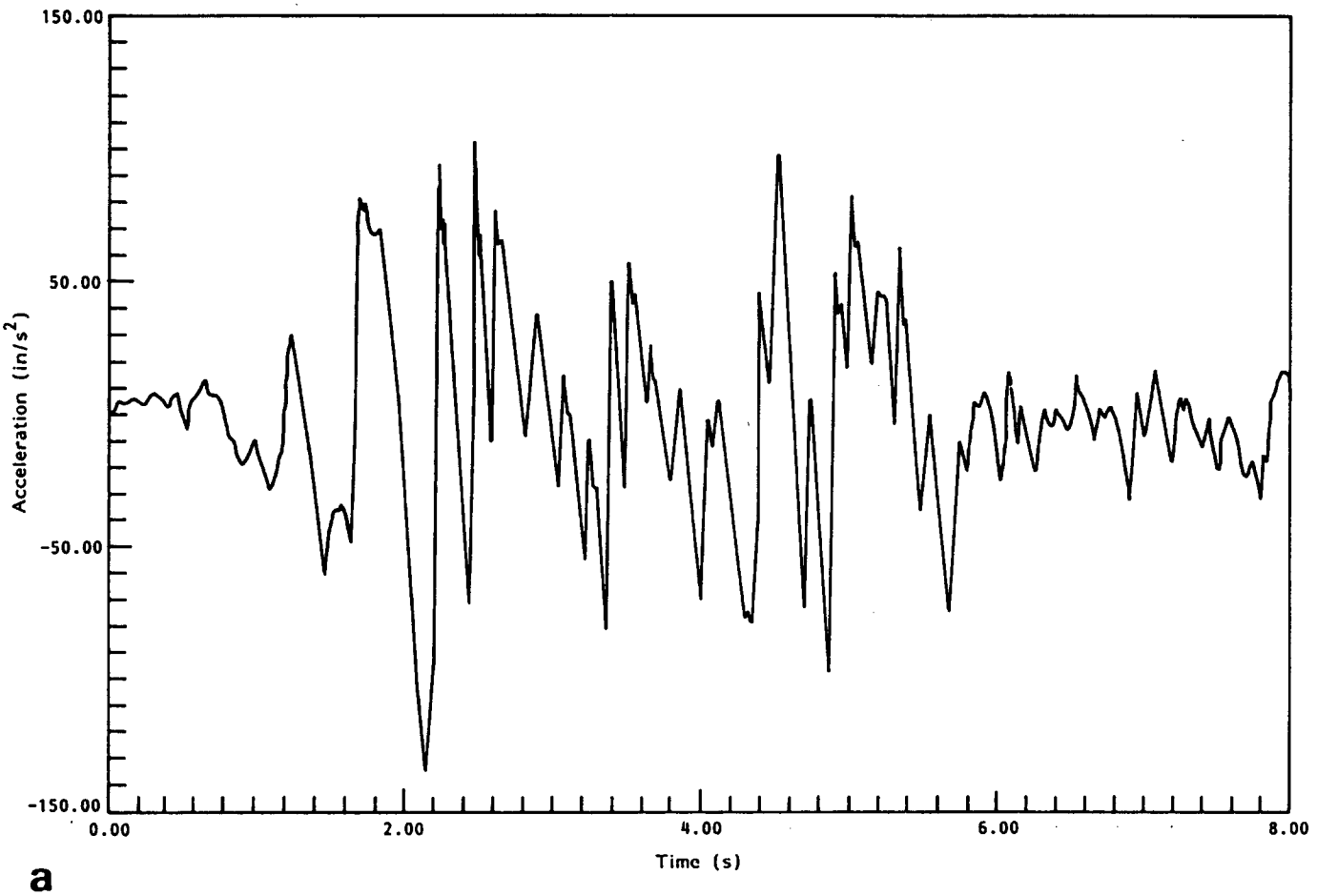

a

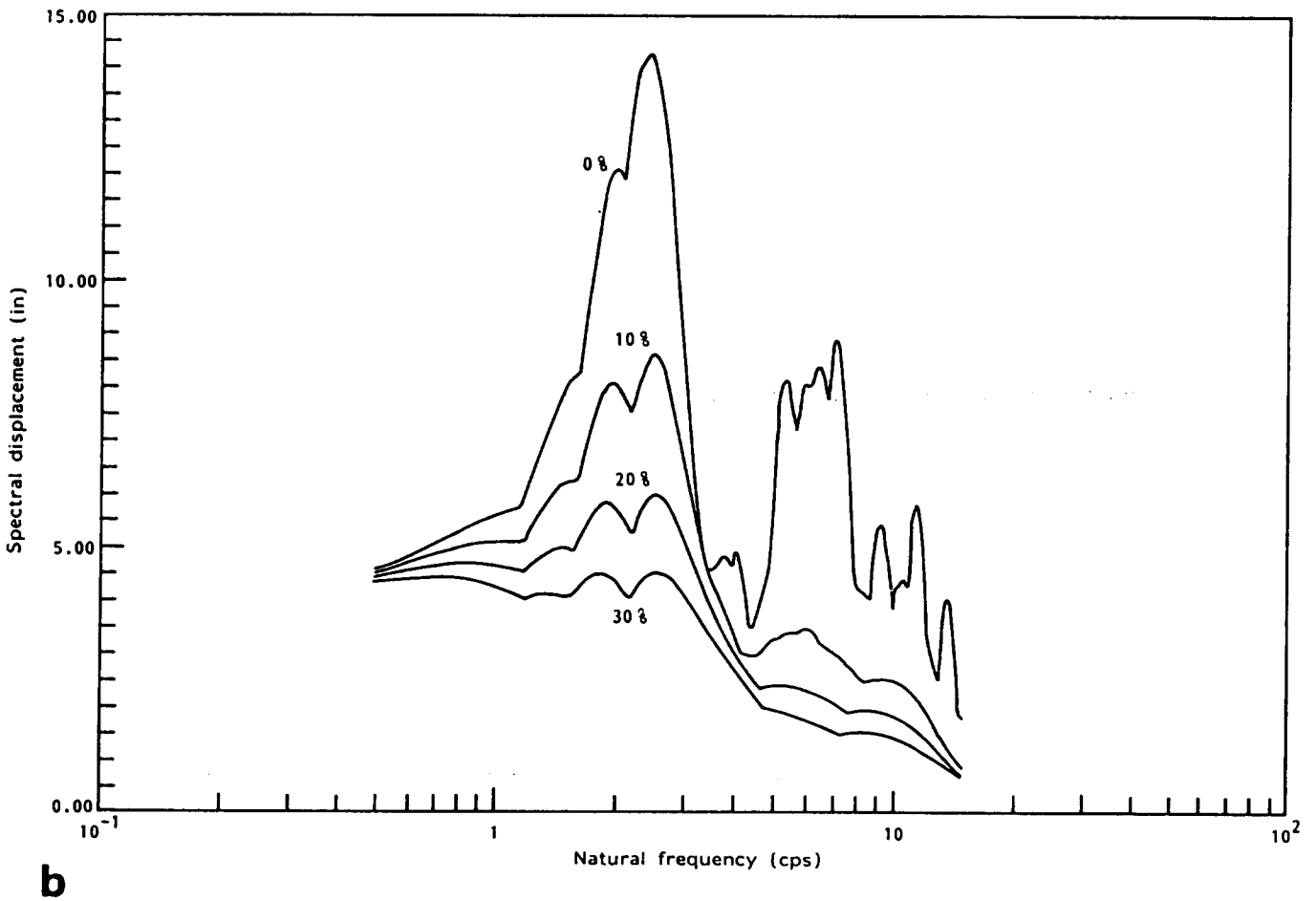

b

Figure 5 (a) El Centro earthquake (1940) acceleration–time history; (b) response spectra for El Centro earthquake

Table 1 Variation of structural parameters

Mass	ρ	Stiffness	E	Height	H
$M0$	$\rho_f = \frac{1}{2}\rho_f^0$ $\rho = \frac{1}{2}\rho^0$	$E0$	$E_f = \frac{1}{4}E_f^0$ $E = \frac{1}{4}E^0$	$H0$	$H = 87.5$ ft
$M1$	$\rho_f = \rho_f^0$ $\rho = \rho^0$	$E1$	$E_f = \frac{1}{2}E_f^0$ $E = \frac{1}{2}E^0$	$H1$	$H = 175$ ft
$M2$	$\rho_f = \frac{3}{2}\rho_f^0$ $\rho = \frac{3}{2}\rho^0$	$E2$	$E_f = E_f^0$ $E = E^0$	$H2$	$H = 262$ ft

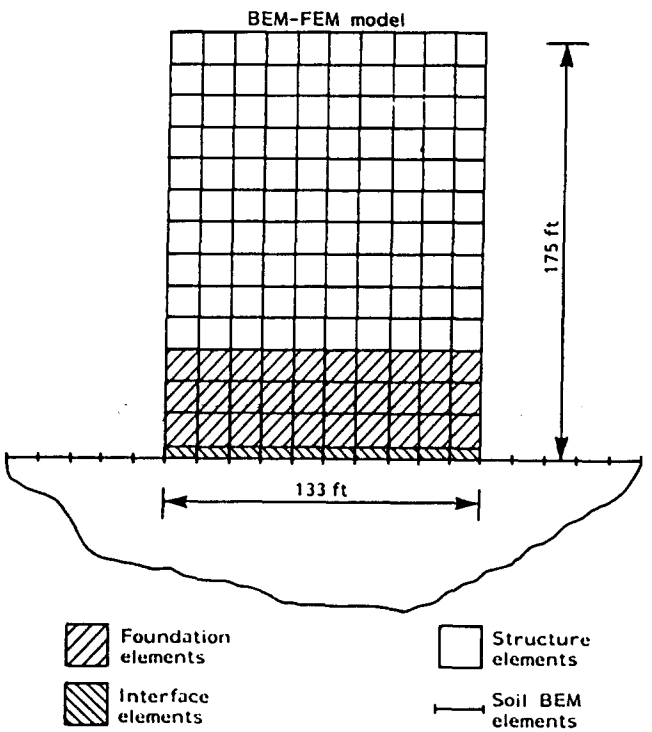

Figure 6 Plane strain BEM-FEM model of nuclear containment structure

discretization has been selected so that the faster c_1 wave travels half the length of the BEM element during a time step, a requirement necessary to secure acceptable solution accuracy[30]. In order to further enhance the solution accuracy, the BEM kernel matrices $[G]$ and $[H]$ in equation (16) have been evaluated on the basis of a further discretization of the 20 elements into five subelements per element. The structure-foundation system is discretized with the aid of FEM into 13 layers of 10 elements across the length of the foundation, hence the soil-foundation interface is also discretized with the aid of 10 interface elements as shown in *Figure 6*. No significant differences in the response time history were observed between the above discretization and a discretization consisting of 15 interface elements with a compatible superstructure FEM mesh, establishing a high level of confidence in the ability of the discretization to accurately predict the correct contact area at the soil-foundation interface.

The horizontal relative response amplitudes at point A for the three models are presented in *Table 2* for the case

Table 2 Comparison of the horizontal relative response amplitudes

	Approximate models		
Mass	Time domain	Frequency domain	BEM-FEM
$M = M1$	1.24 in	1.55 in	1.76 in
$M = M2$	1.56 in	2.32 in	1.86 in
$M = M3$	2.32 in	2.99 in	1.26 in

of complete bond between the soil and foundation. The earthquake acceleration record shown in *Figure 5a* is numerically integrated twice and baseline corrections have been made to obtain displacement-time history for input in the BEM-FEM formulation. The response amplitudes for the frequency domain approximate model are evaluated in two steps: first, the approximate fundamental frequency and the equivalent damping ratio are obtained utilizing equations (31) and (32), and then the amplitudes are determined from the response spectra presented in *Figure 5b*. The time domain amplitudes are obtained directly from the displacement response history calculated for the El Centro earthquake excitation. The magnitudes of the response amplitudes are found to be of the same order as the one evaluated through the rigorous BEM-FEM approach; however, the differences observed are significant. The time domain approximate model appears to underestimate the response amplitudes for all three values of the mass parameter. The frequency domain approach underestimates the response amplitude only for the lowest value of the mass parameter $M0$, and overestimates for the higher values of the mass parameter. Clearly, the approximate models do not necessarily lead to conservative results. In addition, the amplitudes are found to increase monotonically with increase in the mass. Such a behaviour contradicts the non-monotonic behaviour revealed by the rigorous BEM-FEM analysis, indicating the inability of the approximate models to predict the actual changes of the structural behaviour observed when varying the mass parameter.

The absolute horizontal displacement at point A is shown in *Figure 7* for the first six seconds of the earthquake excitation, as it pertains to the strong motion portion of the El Centro earthquake time history. The time domain approximate model appears to give higher response amplitudes than that of the BEM-FEM under

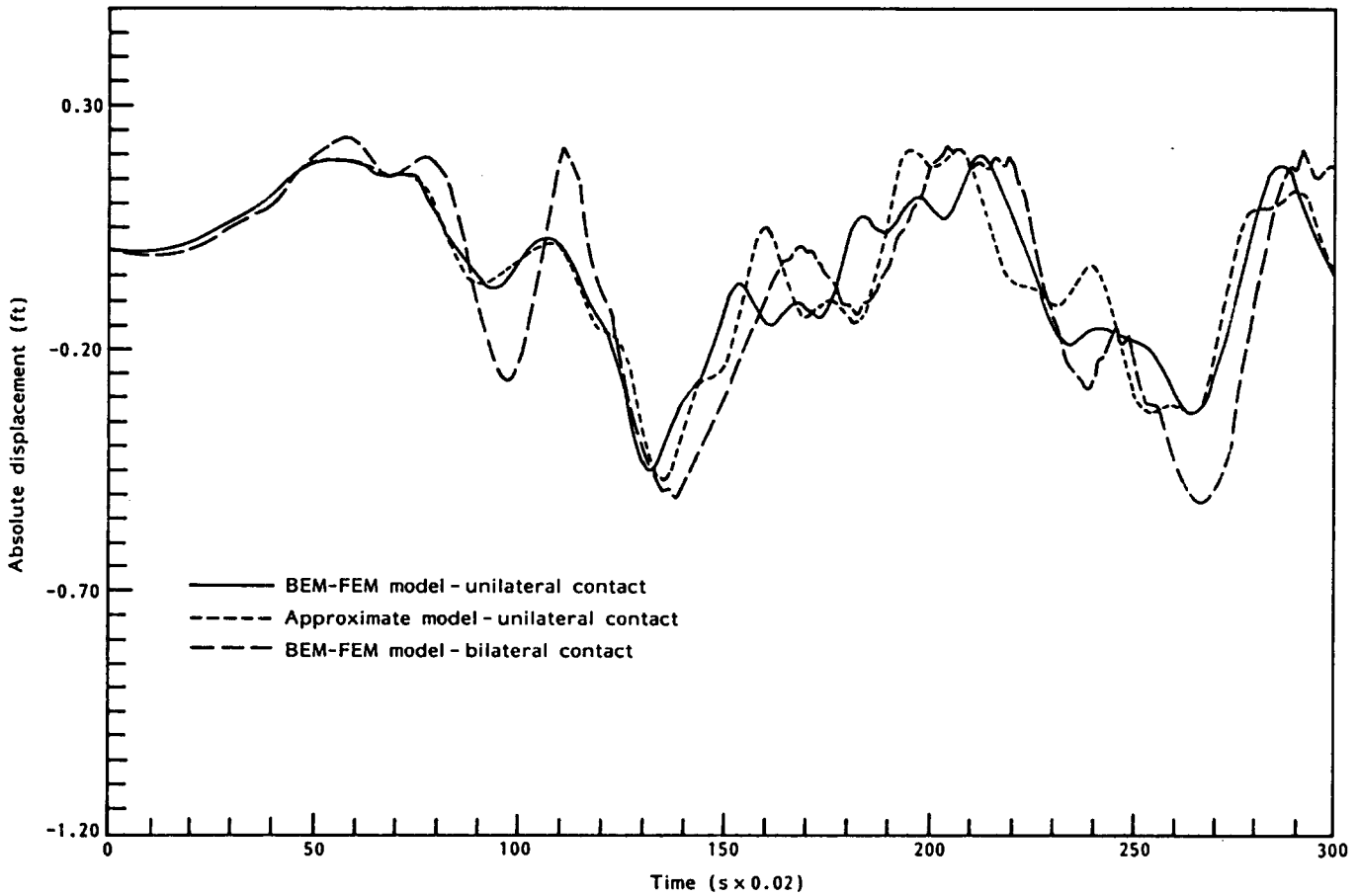

Figure 7 Comparison of the horizontal absolute response at point A

unilateral contact conditions. These differences are expected as the contact area in the approximate model is always overestimated. Also, significant differences are observed between the BEM-FEM response amplitudes due to bilateral and unilateral contact conditions. These differences are better explained from the results shown in *Figure 8*, where the relative displacements at point B are plotted, which shows that the unilateral contact conditions lead to higher amplitudes initially; however, the bilateral contact conditions reveal greater amplitudes at later time steps.

Under bilateral contact conditions the vertical displacement response at point A is shown in *Figure 9* for various values of mass. The displacement amplitude is found to behave non-monotonically with an increase in the value of the mass parameter. Shown in *Figure 10* is the vertical displacement response due to unilateral contact conditions at point A for various values of the mass parameter, a behaviour that significantly differs from the one observed under bilateral contact conditions. It is observed that as the value of the mass increases, the displacement also increases monotonically. This behaviour clearly indicates that one cannot draw conclusions for the nonlinear behaviour under unilateral contact conditions based on the structural behaviour under bilateral contact conditions.

A critical parameter that controls a seismic design is the base shear that develops at the foundation-structure interface. The base shear responses for bilateral and unilateral contact conditions are presented in *Figures 11* and *12*, and the base shear amplitudes are summarized in *Table 3* for all parameter variation. The base shear amplitudes are found to behave non-monotonically with increasing mass for bilateral contact conditions, while their variation is monotonic under unilateral contact conditions. Further, the base shear amplitude is found to substantially increase for certain values of the parameters under unilateral contact conditions. This bahaviour is in agreement with the observations reported by Phycharis and Jennings[7] and Yim and Chopra[9] for structures with low slenderness ratios.

Conclusions

Assuming that only the normal stresses in compression can occur in the area of contact between the foundation and the soil, a hybrid time domain BEM-FEM methodology is developed for the analysis of soil-structure interaction problems in the case of plane strain. The boundary element method is applied to the soil, and the finite element method is applied to the foundation-structure system. FEM interface elements are used to simulate the basemat lift-off during seismic excitation. The methodology leads to nonlinear equations of motion which are solved iteratively utilizing a linear acceleration scheme.

Two approximate models are presented for preliminary design applications of nuclear containment structures. The results are compared with the rigorous BEM-FEM solutions for a representative containment

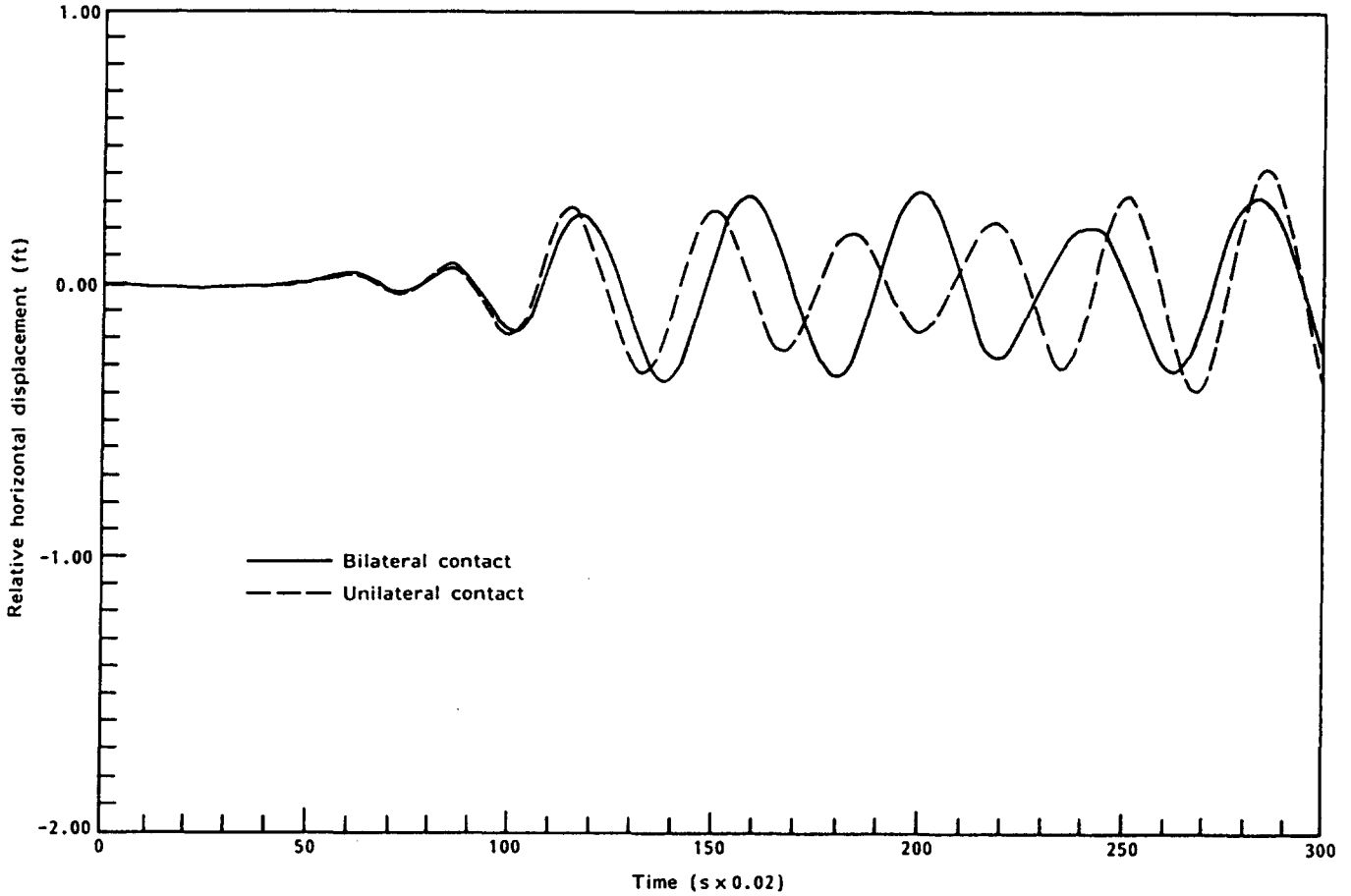

Figure 8 Relative response at point B

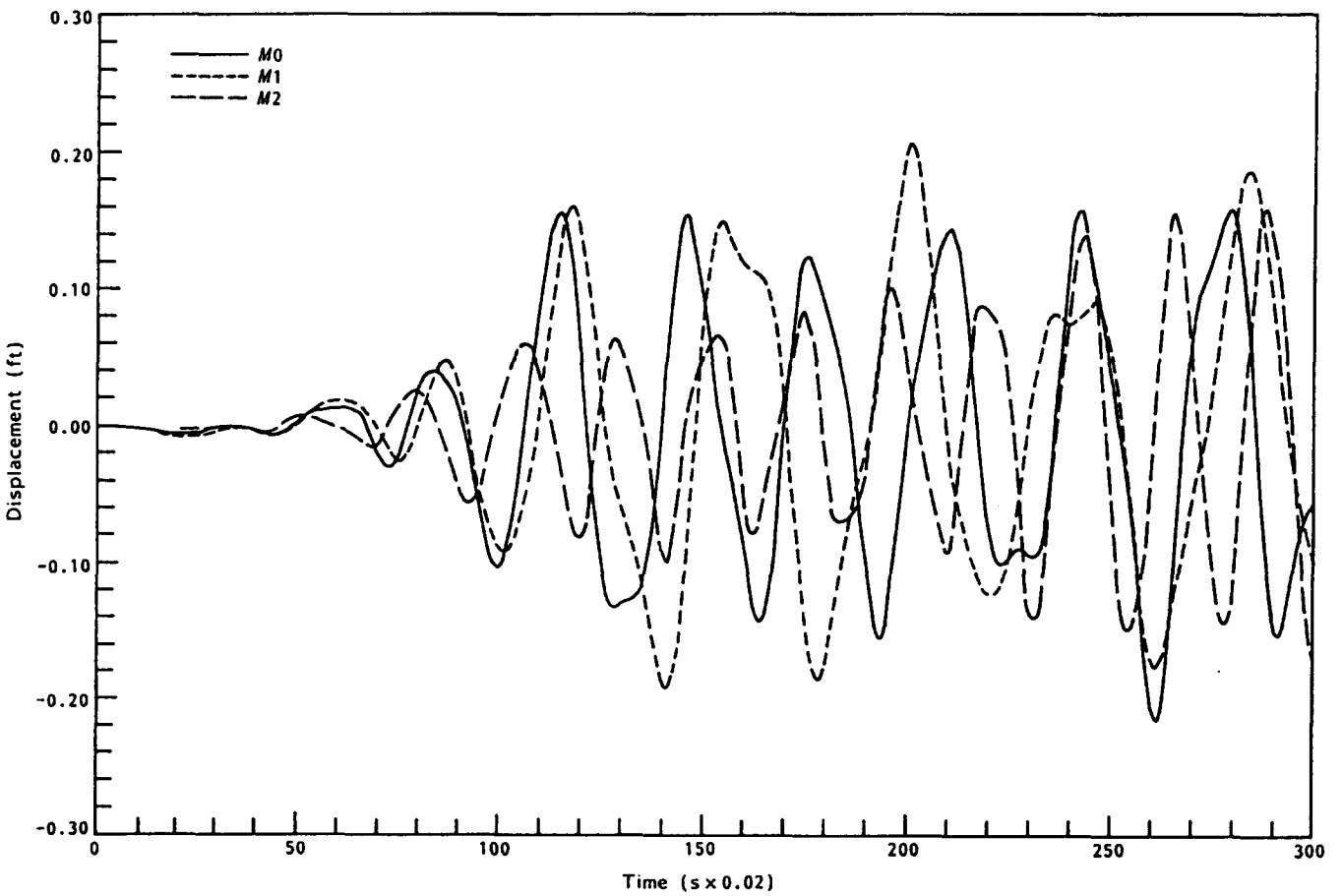

Figure 9 Vertical response at point A—bilateral contact conditions

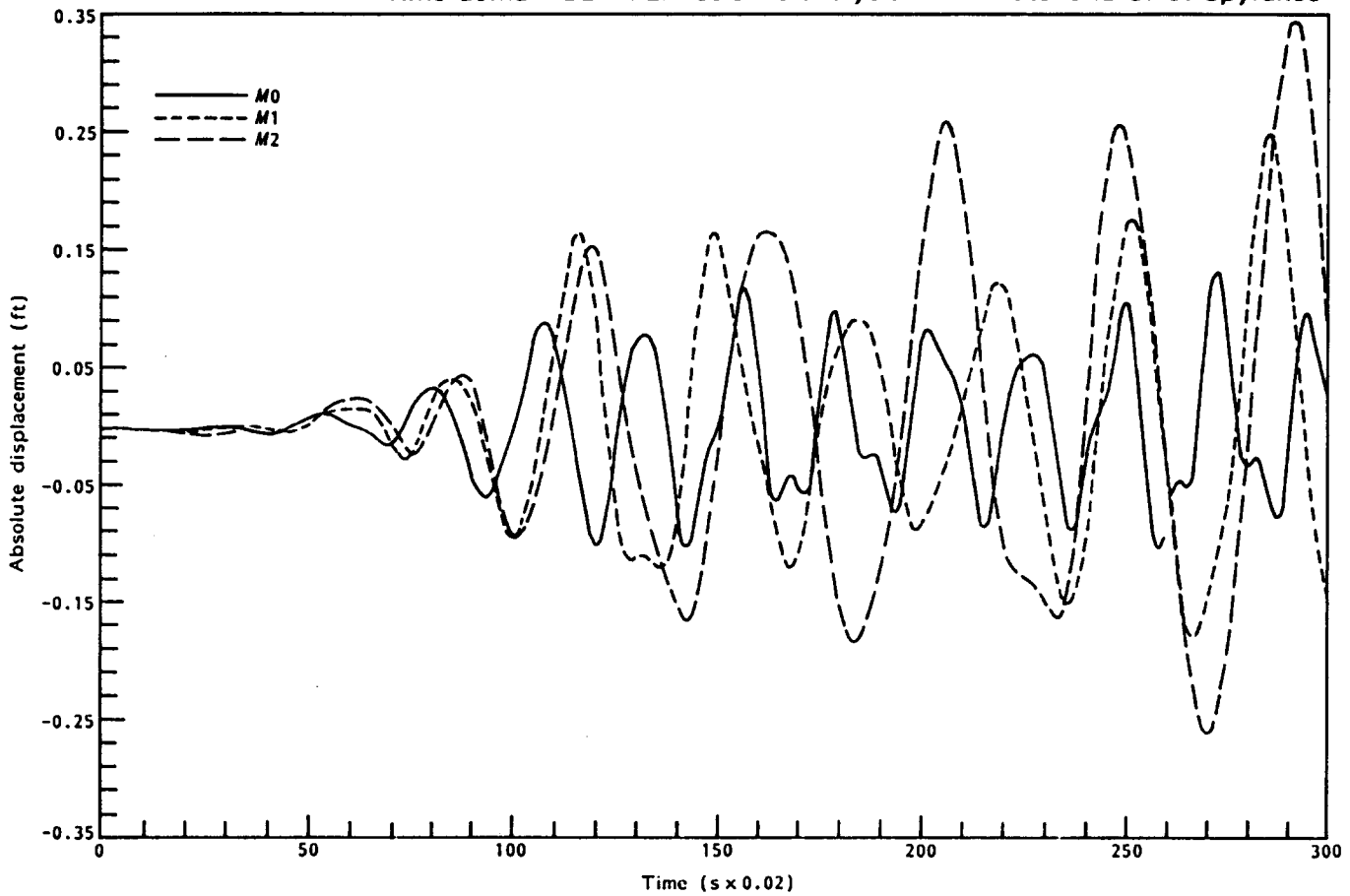

Figure 10 Vertical response at point A—unilateral contact conditions

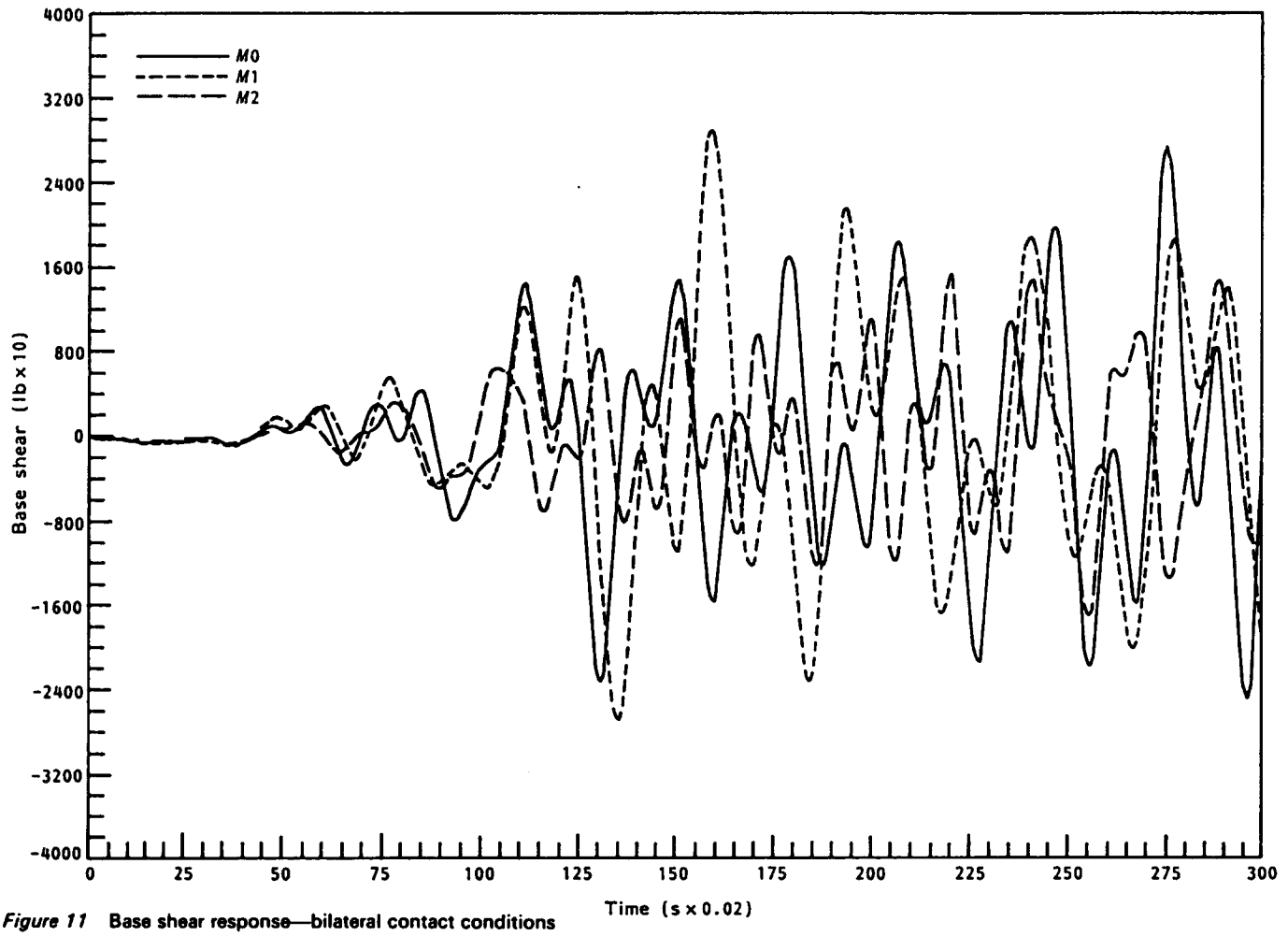

Figure 11 Base shear response—bilateral contact conditions

building subjected to the El Centro earthquake of 1940. The comparison shows that the approximate models can be used to predict the system response amplitudes; however, a comprehensive analysis such as the BEM-FEM approach is required for a complete understanding of the structural behaviour. It should be noted that analyses through approximate models do not necessarily lead to conservative results.

Utilizing the BEM-FEM approach, a parametric study is presented for the parameters that characterize the structural behaviour. The study concludes that for a specific ground excitation, uplift effects on the system response may be malevolent or benevolent depending on the structural parameters. In addition, the effects of uplift on the system response cannot be predicted from the linear behaviour under bilateral contact conditions.

The repeated slamming of the foundation during severe seismic excitations is likely to cause compaction and plastic strains in the soil media surrounding the contact area. A study of these effects could be pursued through an extension of the BEM-FEM methodology presented in this work.

Table 3 Base shear for various parameters—bilateral contact and unilateral contact conditions

Constant parameters	Variable parameters	Base shear (lb) Bilateral contact	Base shear (lb) Unilateral contact
$E = E2$	$M = M0$	27310	14090
$H = H1$	$M = M1$	28970	20130
	$M = M2$	17090	31210
$M = M1$	$E = E0$	25170	31330
$H = H1$	$E = E1$	26720	27630
	$E = E2$	28970	20130
$E = E2$	$H = H0$	23380	45164
$M = M1$	$H = H1$	28970	20130
	$H = H2$	30550	28420

References

1 Hanson, R. D. 'Behavior of liquid-storage tanks'. *The Great Alaska Earthquake of 1964*, Engineering, National Academy of Sciences, Washington, D.C., 1973, 334

2 Housner, G. W. 'The behavior of inverted pendulum structures during earthquakes', *Bull. Seismological Soc. of America*, 1963, **53**, No. 2, 403-417

3 Meek, J. W. 'Effects of foundation tipping on dynamic responses', *J. Struct. Div., ASCE* 1975, **12**, 1297-1311

4 Meek, J. W. 'Dynamic response of tipping core buildings', *Earthquake Engng and Struct. Dyn.* 1978, **6**, 437-454

5 Kennedy, R. P. *et al.* 'Effect of nonlinear soil structure interaction due to base slab uplift on the seismic response of a high-temperature gas-cooled reactor (HTGR)', *Nucl. Engng Design.* 1976, **38**.

6 Huckelbridge, A. A., Jr. and Clough, R. W. 'Seismic response of uplifting building frame', *Proc. ASCE* 1978, ST.8, 1211-1229

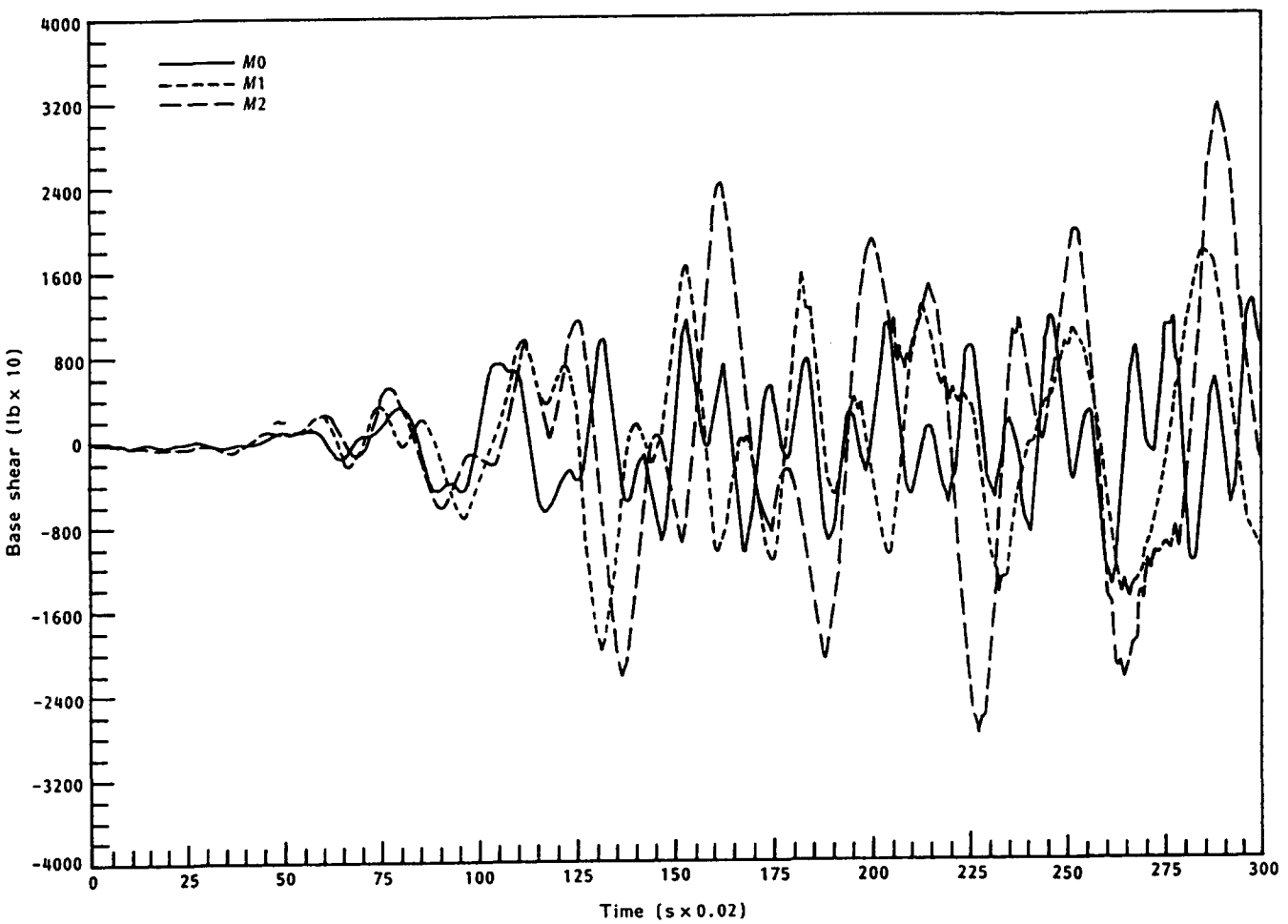

Figure 12 Base shear response—unilateral contact conditions

7 Psycharis, J. N. and Jennings, P. C. 'Rocking of slender rigid bodies allowed to uplift', *Earthquake Engng and Struct. Dyn.* 1983, 11, 57-76

8 Yim, C. S. and Chopra, A. K. 'Earthquake response of structures with partial uplift on Winkler foundation', *Earthquake Engng and Struct. Dyn.* 1984, 12, 263-281

9 Yim, C. S. and Chopra, A. K. 'Simplified earthquake analysis of multistorey structures with foundation uplift', *ASCE J. Struct. Engng.* 1985, 111, No. 12

10 Baba, K. and Nakashima, H. 'Seismic response of uplifting shear wall-flexural frame interaction systems', *Proc. 8th World Conf. on Earthquake Engng*, San Francisco, CA, USA, July 1984

11 Vaughan, D. K. and Isenberg, J. 'Non-linear rocking response of model containment structures', *Earthquake Engng and Struct. Dyn.* 1983, 11, 275-296

12 Roesset, J. M. and Scaletti, 'Nonlinear effects in dynamic soil structure interation', *Third Int. Conf. on Numerical Methods in Geomechanics*, Aachen, FRG, April 1978

13 Wolf, J. P. *et al.* 'Seismic response due to travelling shear wave including soil structure interaction with base mat uplift', *Earthquake Engng and Struct. Dyn.* 1977, 5

14 Weidlinger Associates 'Nonlinear soil structure interaction analysis of SIMQUAKE II', *EPRI Report NP-2353*, April 1982

15 Antes, H. and Steinfeld, B. 'Unilateral contact in dynamic soil-structure interaction by a time domain boundary element method', *Tenth Ann. Conf. on Boundary Element Method*, Computational Mechanics Institute, Southampton, UK, 1988

16 Hillmer, P. and Schmid, G. 'Calculation of foundation uplift effects using a numerical Laplace transform', *Earthquake Engng and Struct. Dyn.* 1988, 16, 789-801.

17 Spyrakos, C. C. and Beskos, D. E. 'Dynamic response of flexible strip-foundation by boundary and finite elements', *Soil Dyn. and Earthquake Engng.* 1986, 5, No. 2, 84-96

18 Karabalis, D. L. and Beskos, D. E. 'Dynamic response of 3-D flexible foundations by time domain BEM and FEM', *Soil Dyn. and Earthquake Engng.* 1985, 4, No. 2, 91-101

19 Banerjee, P. K. and Butterfield, R. *Boundary Elements Methods in Engineering Science*, McGraw-Hill Book Company (UK) Limited, London, 1981

20 Brebbia, C. A., Telles, J. C. and Wrobel, L. C. *Boundary Element Techniques, Theory and Applications in Engineering*, Springer Verlag, Berlin, 1984

21 Erigen, A. C. and Suhubi, E. S. *Elastodynamics Vol. II Linear Theory*, Academic Press, NY, 1975

22 Patel, P. N. 'Localized non-linearities due to soil foundation separation in dynamic soil-structure interation', Dissertation submitted to the College of Engineering of West Virginia University, Morgantown, WV, 1989

23 Bathe, K.-J. *Finite Element Procedures in Engineering Analysis*, Prentice-Hall Inc., Englewood Cliffs, NJ, 1982

24 Zienkiewicz, O. C. *The Finite Element Method*, Third Edition, McGraw-Hall Book Company (UK) Limited, London, 1977

25 Zaman, M. M., Desai, C. S. and Drumm, E. C. 'Interface model for dynamic soil-structure interaction', *J. Geotechnical Engng (ASCE)* 1984, 110, 1257-1273

26 Pande, G. N. and Sharma, K. G. 'On joint/interface elements and associated problems of numerical ill-conditioning', *Int. J. for Numerical and Analytical Methods in Geomechanics.* 1979, 3, 451-457

27 Wilson, E. L., Farhoomand, I. and Bathe, K.-J. 'Nonlinear dynamic analysis of complex structures', *Earthquake Engng and Struct. Dyn.* 1973, 1, 241-252

28 Wolf, J. P. *Dynamic Soil-Structure Interation*, Prentice-Hall Inc., Englewood Cliffs, NJ, 1985

29 Gazetas, G. 'Analysis of machine foundation vibrations: state-of-the-arts', *Soil Dyn. and Earthquake Engng.* 1983, 2, 1-42

30 Spyrakos, C. C., Patel, P. N. and Kokkinos, F. T. 'Assessment of computational practices in dynamic soil-structure interaction', *ASCE J. of Computing in Civ. Engng*, 1989, 3, (2), 143-157

Appendix

Numerical algorithm

A Initial calculations

1) Form stiffness matrix $[\bar{K}]$ and mass matrix $[M]$

$$[\bar{K}_t] = \begin{bmatrix} [K] + [T]^T[B_{cc}][T] & [T]^T[B_{ce}][T] \\ [T]^T[B_{ec}][T] & [T]^T[B_{ee}][T] \end{bmatrix}$$

2) Select time step Δt, parameters α, ρ and calculate integration constants

$$\rho \geq 0.50; \alpha = \geq 0.25(0.5 + \rho)^2$$

$$a_0 = \frac{1}{\alpha \rho t^2}; a_1 = \frac{\rho}{\alpha \Delta t}; a_2 = \frac{1}{\alpha \Delta t}; a_3 = \frac{1}{2\alpha} - 1;$$

$$a_4 = \frac{\rho}{\alpha} - 1; a_5 = \frac{\Delta t}{2}\left(\frac{\rho}{\alpha} - 2\right);$$

$$a_6 = \Delta t(1 - \rho); a_7 \rho \Delta t$$

3) Initializc δ, $\dot{\delta}$, $\ddot{\delta}$ and $\{F^{t-\Delta t}\}$

B For each time step

1) Calculate effective stiffness matrix $[\hat{K}]$

$$[\hat{K}] = [\bar{K}_t] + a_0[M_t]$$

2) Calculate effective loads at time $t + \Delta t$

$$\{\hat{F}^{t-\Delta t}\} = \{F^{t+\Delta t}\} + [M_t](a_0\{\delta^t\} + a_2\{\dot{\delta}^t\} + a_3\{\ddot{\delta}^t\})$$

3) Solve for displacements at time $t + \Delta t$

$$\{\delta\} = [\hat{K}]^{-1}\{\hat{F}^{t+\Delta t}\}$$

4) Check for convergence of the contact area.

(a) If convergence of the contact area is not achieved: calculate new contact area based on $\{\delta^{t-\Delta t}\}$ and new $[K]$ and $[M]$, and start within the same time step at step 1.

(b) If convergence of the contact area is achieved: calculate accelerations and velocities at time $t + \Delta t$.

$$\{\ddot{\delta}^t\} = a_0(\{\delta^{t+\Delta t}\} - \{\delta^t\}) - a_2\{\dot{\delta}^t\} - a_3\{\ddot{\delta}^t\}$$

$$\{\dot{\delta}^t\} = \{\dot{\delta}^t\} + a_6\{\ddot{\delta}^t\} + a_7\{\ddot{\delta}^{T+\Delta t}\}$$

Compute new $[K]$ and $[M]$ and start with new time step at step 1.